Measurement of Electron-Neutrino Charged-Current Cross Sections on ^{127}I with the COHERENT NaIνE Detector

P. An,[1,2,*] C. Awe,[1,2] P. S. Barbeau,[1,2] B. Becker,[3] V. Belov,[4,5] I. Bernardi,[3] C. Bock,[6] A. Bolozdynya,[4] R. Bouabid,[1,2]
A. Brown,[7,2] J. Browning,[8] B. Cabrera-Palmer,[9] M. Cervantes,[1] E. Conley,[1] J. Daughhetee,[10] J. Detwiler,[11] K. Ding,[6]
M. R. Durand,[11] Y. Efremenko,[3,10] S. R. Elliott,[12] L. Fabris,[10] M. Febbraro,[10] A. Gallo Rosso,[13] A. Galindo-Uribarri,[10,3]
A. C. Germer,[14] M. P. Green,[2,10,8] J. Hakenmüller,[1] M. R. Heath,[10] S. Hedges,[1,2,†,‡] M. Hughes,[15] B. A. Johnson,[15]
T. Johnson,[1,2] A. Khromov,[4] A. Konovalov,[4,§] E. Kozlova,[4] A. Kumpan,[4] O. Kyzylova,[16] L. Li,[1,2] J. M. Link,[16] J. Liu,[6]
M. Mahoney,[14] A. Major,[1] K. Mann,[8] D. M. Markoff,[7,2] J. Mastroberti,[15] J. Mattingly,[17] P. E. Mueller,[10] J. Newby,[10]
D. S. Parno,[14] S. I. Penttila,[10] D. Pershey,[1] C. G. Prior,[1,2] R. Rapp,[18] H. Ray,[19] J. Raybern,[1] O. Razuvaeva,[4,5]
D. Reyna,[9] G. C. Rich,[2] J. Ross,[7,2] D. Rudik,[4,‖] J. Runge,[1,2] D. J. Salvat,[15] J. Sander,[6] K. Scholberg,[1] A. Shakirov,[4]
G. Simakov,[4,5] G. Sinev,[1,¶] C. Skuse,[14] W. M. Snow,[15] V. Sosnovtsev,[4] T. Subedi,[16,20] B. Suh,[15] R. Tayloe,[15]
K. Tellez-Giron-Flores,[16] Y.-T. Tsai,[21] E. Ujah,[7,2] J. Vanderwerp,[15] E. E. van Nieuwenhuizen,[1,2] R. L. Varner,[10]
C. J. Virtue,[13] G. Visser,[15] K. Walkup,[16] E. M. Ward,[3] T. Wongjirad,[22] J. Yoo,[23] C.-H. Yu,[10] A. Zawada,[2]
J. Zettlemoyer,[15,**] and A. Zderic[11]

[1]*Department of Physics, Duke University, Durham, North Carolina 27708, USA*
[2]*Triangle Universities Nuclear Laboratory, Durham, North Carolina 27708, USA*
[3]*Department of Physics and Astronomy, University of Tennessee, Knoxville, Tennessee 37996, USA*
[4]*National Research Nuclear University MEPhI (Moscow Engineering Physics Institute), Moscow 115409, Russian Federation*
[5]*National Research Center "Kurchatov Institute," Moscow, 123182, Russian Federation*
[6]*Department of Physics, University of South Dakota, Vermillion, South Dakota 57069, USA*
[7]*Department of Mathematics and Physics, North Carolina Central University, Durham, North Carolina 27707, USA*
[8]*Department of Physics, North Carolina State University, Raleigh, North Carolina 27695, USA*
[9]*Sandia National Laboratories, Livermore, California 94550, USA*
[10]*Oak Ridge National Laboratory, Oak Ridge, Tennessee 37831, USA*
[11]*Center for Experimental Nuclear Physics and Astrophysics and Department of Physics, University of Washington, Seattle, Washington 98195, USA*
[12]*Los Alamos National Laboratory, Los Alamos, New Mexico 87545, USA*
[13]*Department of Physics, Laurentian University, Sudbury, Ontario P3E 2C6, Canada*
[14]*Department of Physics, Carnegie Mellon University, Pittsburgh, Pennsylvania 15213, USA*
[15]*Department of Physics, Indiana University, Bloomington, Indiana 47405, USA*
[16]*Center for Neutrino Physics, Virginia Tech, Blacksburg, Virginia 24061, USA*
[17]*Department of Nuclear Engineering, North Carolina State University, Raleigh, North Carolina 27695, USA*
[18]*Washington & Jefferson College, Washington, Pennsylvania 15301, USA*
[19]*Department of Physics, University of Florida, Gainesville, Florida 32611, USA*
[20]*Department of Physical and Environmental Sciences, Concord University, Athens, West Virginia 24712, USA*
[21]*SLAC National Accelerator Laboratory, Menlo Park, California 94025, USA*
[22]*Department of Physics and Astronomy, Tufts University, Medford, Massachusetts 02155, USA*
[23]*Department of Physics and Astronomy, Seoul National University, Seoul, 08826, Korea*

Using an 185-kg NaI[Tl] array, COHERENT has measured the inclusive electron-neutrino charged-current cross section on ^{127}I with pion decay-at-rest neutrinos produced by the Spallation Neutron Source at Oak Ridge National Laboratory. Iodine is one the heaviest targets for which low-energy (≤ 50 MeV) inelastic neutrino-nucleus processes have been measured, and this is the first measurement of its inclusive cross section. After a five-year detector exposure, COHERENT reports a flux-averaged cross section for electron neutrinos of $9.2^{+2.1}_{-1.8} \times 10^{-40}$ cm^2. This corresponds to a value that is ~41% lower than predicted using the MARLEY event generator with a measured Gamow-Teller strength distribution. In addition, the observed visible spectrum from charged-current scattering on ^{127}I has been measured between 10 and 55 MeV, and the exclusive zero-neutron and one-or-more-neutron emission cross sections are measured to be $5.2^{+3.4}_{-3.1} \times 10^{-40}$ and $2.2^{+3.5}_{-2.2} \times 10^{-40}$ cm^2, respectively.

Introduction.—There are little existing experimental data on low-energy inelastic neutrino-nucleus scattering. For terrestrial-based neutrinos with energy less than 100 MeV, measurements exist for only seven nuclear targets [1–3]. Despite the dearth of experimental data, there are motivations for the study of these interactions in detecting solar and supernova neutrinos [4], improving our understanding of weak interactions with the nucleus [5], and quantifying backgrounds for neutrino-scattering experiments.

Inelastic charged-current (CC) neutrino interactions on ^{127}I (ν_eCC-^{127}I), in particular, have generated interest for solar and supernova neutrino detection. The low Q value (662.3 keV) for the ν_eCC-^{127}I interaction, along with the large predicted cross section and long half-life of the resulting ^{127}Xe nucleus, make iodine a promising target for radiochemical neutrino detection. Recent calculations [6] have shown that, by measuring the fraction of ν_eCC-^{127}I events that emit a neutron, an ^{127}I solar neutrino detector can provide information on the fluxes of different types of solar neutrinos.

In existing calculations, there are large variations of the pion decay-at-rest (π-DAR) flux-averaged ν_eCC-^{127}I cross section [5,7–9]. One factor impacting predictions is the weak axial-vector coupling constant g_A. By measuring exclusive cross sections to specific multipoles in the resulting ^{127}Xe nucleus, it may be possible to learn about the quenching of g_A [5]. Neutrino-nucleus interactions at π-DAR sources allow the study of g_A in a weak process at larger momentum transfer ($Q \sim 10$ s of MeV/c) than is achievable through β-decay experiments ($Q \sim 1$ MeV/c). The dependence of g_A on momentum transfer has a large impact on neutrinoless double beta-decay ($0\nu\beta\beta$) experiments, where the $0\nu\beta\beta$ half-life depends on g_A to the fourth power. A review of the g_A quenching problem and its impact on $0\nu\beta\beta$ matrix elements can be found in Ref. [10].

In searches for coherent elastic neutrino-nucleus scattering (CEνNS), inelastic neutrino-nucleus interactions occurring in the active detector volume or surrounding shielding can form a background [11]. Neutrino interactions can produce excited nuclear states that deexcite by emitting neutrons. Neutrino-induced neutrons (NINs) can produce keV-scale nuclear recoils that mimic the CEνNS signal. Additionally, NINs are one of the only backgrounds that can follow the timing distribution of neutrinos produced by pulsed spallation neutron sources. COHERENT plans to measure CEνNS on ^{23}Na using a tonne-scale NaI[Tl] scintillator array. NINs from ν_eCC-^{127}I can form a background for this search. While the CEνNS cross section on ^{23}Na is expected to be larger than the ν_eCC-^{127}I cross section, the exclusive ν_eCC-^{127}I channel leading to neutron emission on iodine has never been measured. A recent search for NINs on ^{208}Pb observed a cross section substantially lower than existing theoretical predictions, although the source of this suppression is unknown [3].

The exclusive ν_eCC-^{127}I channel to bound states of ^{127}Xe (referred to as $0n$) was measured for π-DAR neutrinos by E-1213 at the Los Alamos Meson Physics Facility (LAMPF) [12]. By extracting ^{127}Xe produced in a 1540-kg NaI solution and counting its decay, a flux-averaged exclusive cross section of $[2.84 \pm 0.91(\text{stat}) \pm 0.25(\text{syst})] \times 10^{-40}$ cm^2 was reported. The radiochemical approach was insensitive to CC interactions leading to the emission of one or more neutrons ($\geq 1n$), while the majority of ν_e emitted at a π-DAR source have energies above the neutron emission threshold of 7.246 MeV [6]. Additionally, radiochemical approaches are unable to measure the energy dependence of the ν_eCC-^{127}I cross section.

The NaI Neutrino Experiment (NaIνE) was deployed by the COHERENT Collaboration to the Spallation Neutron Source (SNS) at Oak Ridge National Laboratory (ORNL) to measure the inclusive ν_eCC-^{127}I cross section. Details on the detector, calibrations, signal predictions, and results from a five-year search are presented here.

Experimental description.—The NaIνE detector consists of 24 2" × 4" × 16" NaI[Tl] scintillator crystals, each with a mass of ~7.7 kg, enveloped in thin aluminum shielding. The crystals are arranged in a 4 × 6 array, oriented vertically, as depicted in Fig. 1. Each crystal is equipped with a ten-stage 3.5" diameter Burle S83013 photomultiplier tube (PMT). Two-inch plastic scintillator muon veto panels tag muon backgrounds, and 1.5" of A36 steel rests between the NaI[Tl] crystals and vetoes to avoid vetoing the CC signal. The side (top) veto panels are equipped with two (four) ET-9078B PMTs. The detector began operating at the SNS in its current shielding configuration in 2017.

The detector is located in a basement hallway at the SNS target station, 18.7 m from the SNS mercury target, where it is exposed to an intense flux of π-DAR neutrinos (~5.4×10^7 cm^{-2} s^{-1} at 18.7 m) [13]. At the SNS, ν_e is
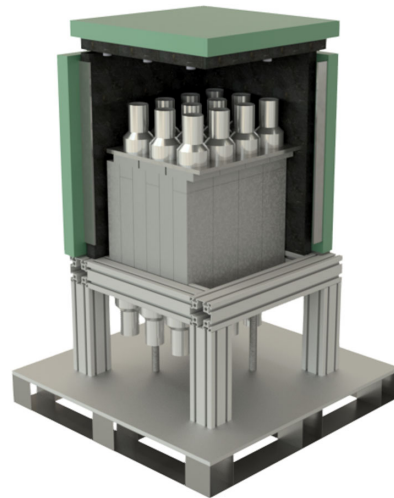

FIG. 1. Cutaway view of the 24-crystal NaIνE detector. Muon veto panels are depicted in green and steel shielding in dark gray.

the only flavor that can undergo CC interactions, as the muon-neutrino energy is too low to produce muons. The timing of the ν_e flux is determined by the 350 ns FWHM proton-on-target (POT) pulse convolved with the 26 ns mean lifetime of the pion and the 2.2 μs mean lifetime of the muon. The maximum energy of the produced ν_e is ~52.8 MeV. Additional details on neutrino production at the SNS can be found in Ref. [13].

The 24 NaI[Tl] PMTs, 12 muon veto PMTs, and two timing channels from the SNS are read out using five Struck SIS3302 digitizers [eight channels, 100 MHz, 16-bit analog-to-digital converter (ADC)]. Each channel triggers independently using a moving-average trapezoidal trigger. The NaI[Tl] channel trigger thresholds range from 500 to 900 keV. To reduce the amount of data generated, digitizers store the integrated PMT signal in eight 1.25-μs windows around the triggering pulse. The first two windows record the baseline level, and the following three integrate pulse signal to define an energy quantity. The digitizer additionally records the peak ADC value of the pulse, the location of the peak within the 10-μs trace, and whether there is pileup from additional triggers. In analysis, NaI[Tl] signals are correlated with veto and POT signals. One malfunctioning NaI[Tl] crystal was removed from analysis but remained *in situ* and was simulated.

Energy depositions from multiple NaI[Tl] detectors are grouped to form events if they occur within a 400-ns time window. Long coincidence windows are not atypical for other large NaI[Tl] arrays [14,15].

NaI[Tl] scintillator events are associated with cosmic muon events if they occur within a $[-6 \text{ μs}, +20 \text{ μs}]$ window around a muon veto PMT signal. The thresholds for the muon vetoes range from 300 to 700 keV.

Data occurring within a $[-2 \text{ μs}, +20 \text{ μs}]$ window of the POT pulse were blinded to avoid biasing cuts. Health checks removed periods of operation with irregular SNS beam operations or detector electronics issues.

Detector calibration.—While NaI[Tl] scintillators are known to exhibit a nonlinear light yield below 1 MeV [16], the high-energy light yield is fairly linear [17]. Each NaI[Tl] detector was calibrated in two steps, first using peaks from low-energy gamma backgrounds, followed by high-energy Michel positrons to account for nonlinearities in the light yield and PMT response. The low-energy calibrations use events from ^{40}K (^{208}Tl) at 1.461 (2.615) MeV to estimate the energy scale and track gain changes that occur due to PMT aging and temperature fluctuations. The higher-energy calibrations identify Michel positron candidates by searching to 10-to-55 MeV depositions following a tagged muon-veto event and is applied to ensure the detector energy response is correct in the energy region of interest (ROI) relevant for CC events in this analysis. Additional details on the calibrations can be found in Supplemental Material [18].

To avoid threshold effects, a software cut removes energy depositions in any crystal below 1 MeV so that the trigger efficiency is ~100%. A second cut removes events with an energy deposition in a single crystal greater than 55 MeV, as these are outside the ν_eCC-^{127}I ROI.

Simulation and signal prediction.—All CC event generation was done with MARLEY [19]. Although designed for CC interactions on ^{40}Ar [20], MARLEY has been adapted for use with other nuclei. MARLEY simulates the allowed component of neutrino-nucleus interactions, relying on provided distributions of the Gamow-Teller (GT$^-$) and Fermi (F) strengths. For iodine, B(GT$^-$) data are obtained from the charge-exchange experiment in Ref. [21]. Similarly, B(GT$^-$) data in Refs. [22,23] were used for ^{23}Na CC events originating in the NaI[Tl] detectors and ^{56}Fe CC events originating in the shielding. An extended discussion of MARLEY's predictions for ^{127}I can be found in [18]. The predicted flux-averaged ν_eCC-^{127}I cross section from MARLEY is $22.5^{+1.2}_{-6.5} \times 10^{-40}$ cm^2, with uncertainties originating from those provided in the measured GT strength distribution.

One of the key signatures of CC interactions at π-DAR sources is the delayed timing of electron neutrinos resulting from the 2.2 μs muon lifetime. This timing distribution is not affected by uncertainties associated with forbidden transitions or g_A quenching, so these factors predominantly affect the predicted spectral shape from MARLEY. The amplitude of the ν_eCC-^{127}I component is allowed to float in our fits. Backgrounds from neutrino-electron scattering were ignored, as their expected rate is only 1.2% of the expected ν_eCC-^{127}I signal.

A GEANT4 [24] simulation was used to simulate detector response Michel positrons, beam-related neutrons (BRNs), and CC events on ^{127}I, ^{23}Na, and ^{56}Fe. Simulations were postprocessed with cuts designed to match those applied to detector data. Energy smearing was applied to simulated events using the measured energy resolution from the detector calibrations. While nuclear recoils from CC interactions and neutron interactions are below detector thresholds, they are included, along with nuclear recoil quenching factors [25], as they can produce in shifts in the reconstructed energy. The predicted energy distributions in NaIνE (with arbitrary normalization) from simulation are shown in Fig. 2.

The neutrino flux normalization was parametrized as a function of proton power and energy using a simulation from Ref. [13], with a 10% normalization uncertainty. The spectral shape of electron neutrinos from muon decay is well known [26]. Using the MARLEY cross sections, the signal expectations over the 22.8-GWhr exposure for events with visible energy between 10 and 55 MeV are ~1320 CC events on ^{127}I and ~61 CC events from ^{23}Na and ^{56}Fe. The expected rates for the prompt neutron background were taken from Ref. [3].
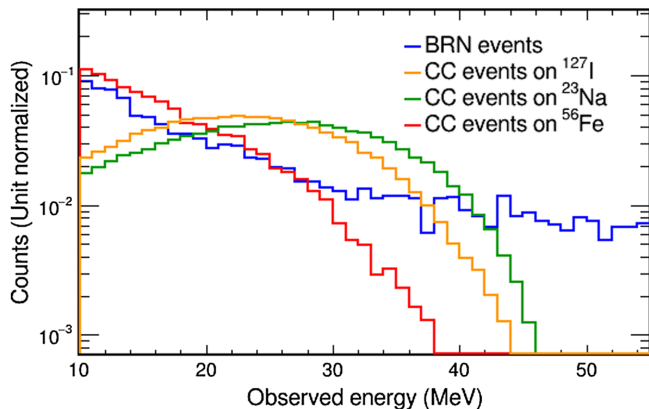
FIG. 2. Simulated visible energy spectra of ^{127}I CC (orange line), ^{23}Na CC (green line), ^{56}Fe CC (red line), and beam-related neutron signals (blue line), after applying cuts. Amplitudes of each component are normalized to unity.

FIG. 3. The observed NaIνE timing spectrum compared to the total prediction, with an inset showing the background-subtracted timing distribution. The CC spectrum with 1σ uncertainty from the 1D fit is also shown along with the nominal MARLEY prediction and steady-state, BRN, and Na + Fe CC backgrounds.

Prior to unblinding, the neutron rate and timing shape were studied in low-energy (7–8 MeV) and high-energy (55–100 MeV) sidebands to validate the BRN simulation. A one-dimensional binned-timing fit was performed on both of these samples, allowing the neutron normalization and arrival time to float. Additionally, to accommodate differences in time of flight for neutrons of different energy, the timing width was allowed to float by convolving the POT timing distribution with a Gaussian of parametrized width. The neutron rate at the NaIνE location was higher than expected by factor of 6.3 and 9.8 in the respective low- and high-energy sidebands [3]. Neutrons in the high-energy sideband were observed 53 ± 6 ns earlier than those in the low-energy sideband. Furthermore, while the high-energy sideband data were consistent with the POT pulse width, the low-energy data preferred a 33 ± 9 ns additional time broadening. These differences are not understood, but we suspect they are due to lower-energy secondary interactions that can be produced by higher-energy neutrons. Because of these differences, the neutron amplitude, timing offset, and additional width were allowed to float independently in every energy bin. Thus, we made no prior assumption on the neutron energy or timing distribution.

Results and discussion.—The data analysis was blinded with all choices of event selection and fitting finalized before the data were analyzed. Beam events were selected, and the observed energy and timing were reconstructed. Event timing is the principal discriminator between CC and prompt neutron background as ν_e CC events are delayed from the POT onset.

To mitigate uncertainties from the model of the prompt neutron energy spectrum, the total ν_eCC-^{127}I cross section was determined by a binned 1D timing fit. Events with observed energy below 10 MeV were excluded from the fit to reject neutron capture events (most intense between 4.5 and 6.8 MeV [27,28]) which are delayed at a timescale of several microseconds. Additionally, events above 55 MeV
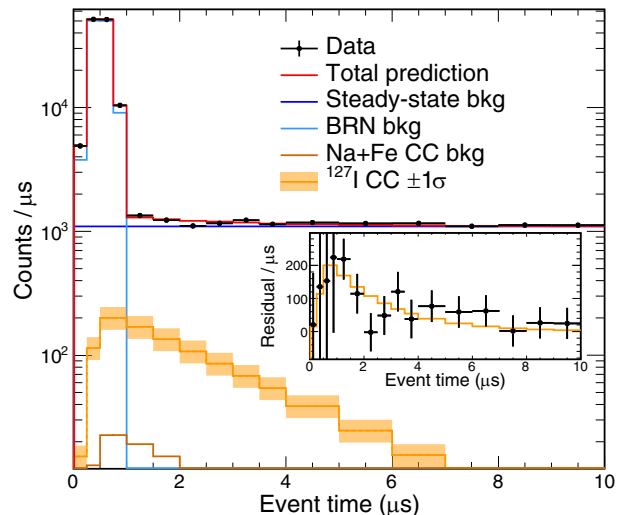
were removed, as these events are beyond the π-DAR end point energy.

The systematic uncertainty on the ^{127}I CC normalization was 11.4%, dominated by the neutrino flux uncertainty of 10%. This includes a 5.1% uncertainty on the fraction of CC events that are rejected by the muon veto panels—this uncertainty originates from the spatial dependence on the threshold within the veto, and its impact was studied through simulation. We also include uncertainties on the calibration, energy resolution, and neutrino interaction modeling which contribute each $< 1\%$.

The steady-state background prediction (predominantly cosmic rays that did not trigger the veto system) was measured *in situ* with out-of-beam-window data, with negligible uncertainty on its normalization. The prompt neutron flux, arrival time, and timing width were allowed to float without any prior constraint. We included a $\pm 100\%$ uncertainty on the normalization of background ^{23}Na and ^{56}Fe CC due to large cross-section uncertainty. This introduces an uncertainty on the ^{127}I event rate by 31 and 30 events for ^{23}Na and ^{56}Fe, respectively.

After selection, we calculated the likelihood curve as a function of the number of ^{127}I CC events while profiling systematic uncertainties. With this, we find a best fit and 1σ range of 541^{+121}_{-108}, corresponding to a flux-averaged cross section of $(9.2^{+2.1}_{-1.8}) \times 10^{-40}$ cm^2 and inconsistent with the background-only hypothesis at 5.8σ. The best-fit timing spectrum is shown in Fig. 3 and has a χ^2 per degree of freedom of 13.1/11. The best-fit normalization is only 40.9% of the MARLEY expectation, similar to the NIN suppression COHERENT has observed in lead [3]. While disparate from MARLEY's prediction, the measured inclusive cross section is closer to predictions in Ref. [7]
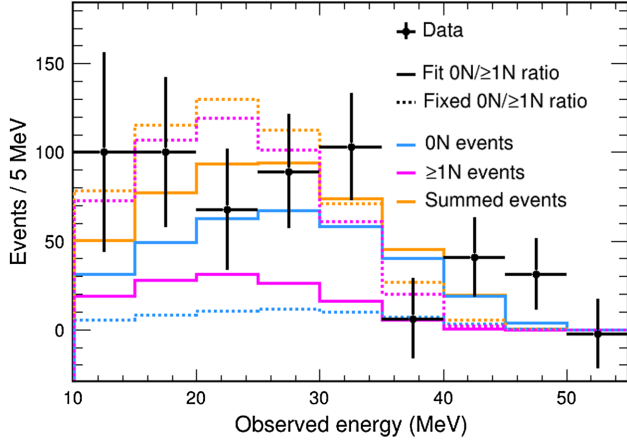
FIG. 4. The visible energy spectrum of CC events between 10 and 55 MeV is shown in black, along with the best-fit spectrum from MARLEY (orange) allowing the $\geq 1n$ and $0n$ amplitudes to float.

$(7.3 \times 10^{-40}$ cm$^2)$ and Ref. [9] $(12.5 \times 10^{-40}$ cm$^2)$. MARLEY's prediction is generated using an assumption of an unquenched g_A (see Supplemental Material [18]), and, while the MARLEY model neglects forbidden transitions, we set an upper bound on the suppression of the GT interaction strength for ν_eCC-^{127}I scattering with π-DAR neutrinos of ≤ 0.59, corresponding to $g_{A,\text{eff}} \leq 0.97$. This upper limit is derived from the lower 1σ uncertainty on the GT matrix elements in Ref. [21] and the upper 1σ uncertainty on the measured cross section.

We investigate the exclusive channel by considering the energy dependence of NaIνE data due to differences in nuclear binding energy to compare to the measurement of ^{127}I$(\nu_e, e^-)^{127}$Xe at LAMPF [12] which determined a cross section of $[2.84 \pm 0.91(\text{stat}) \pm 0.25(\text{syst})] \times 10^{-40}$ cm^2. The $1n$ emission threshold is ~7 MeV larger than that of the $0n$ channel and much larger than detector resolution. After applying detector resolution, the 40–50 MeV range is sensitive to $0n$ events, while the $\geq 1n$ channel is kinematically forbidden.

We performed a 2D fit in time and energy to constrain the $0n$ and $\geq 1n$ event normalizations with NaIνE data. As
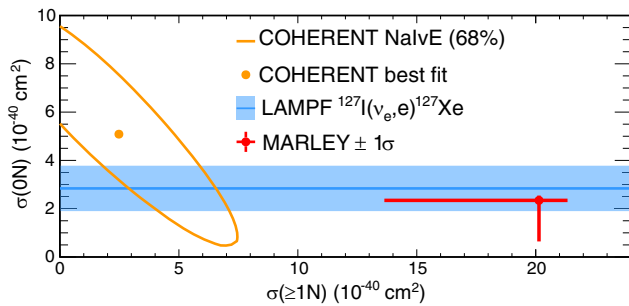

FIG. 5. Measurement (1σ) of the ν_eCC-^{127}I cross section separated into $0n$ and $\geq 1n$ channels compared to the MARLEY prediction and Ref. [12], measuring the $0n$ cross section.

previously described, the prompt neutron energy distribution is known to be mismodeled, and, thus, the neutron normalization and timing is floated in each energy bin independently. The 2D fit is susceptible to uncertainties on the MARLEY predictions for the shape of the observed energy distribution; however, the relative fraction of $0n$ and $\geq 1n$ events dominate spectral distortions. Thus, we introduce only two uncorrelated fit parameters: the amplitude of $0n$ and $\geq 1n$ events. Additionally, the bias introduced on the cross sections is much smaller than statistical uncertainty in this measurement. These effects will be included in a future measurement from the NaI[Tl] Neutrino Experiment TonnE-scale (NaIνETe) 3.5-tonne detector, currently being deployed at the SNS, which will dramatically reduce statistical errors.

The resulting energy distribution from the 2D fit is shown in Fig. 4. The fit agrees well with the model, $\chi^2/\text{d.o.f.} = 147.3/139$. Interestingly, the fit prefers a much higher fraction of $0n$ events (72.3%) than MARLEY predicts (10.6%), though this preference is not strong (a $\Delta\chi^2 = 3.3$ between the best fit and the MARLEY $0n$ fraction). Further data collected with the COHERENT NaIνE and NaIνETe detectors can be used to investigate the cross sections of these exclusive channels to tune event generators for CC interactions on heavy nuclei at energies relevant for π-DAR, solar, and supernova neutrino measurements.

From the 2D fit, we derive measurements of the cross sections to the exclusive $0n$ and $\geq 1n$ channels simultaneously. Our measurement is shown in Fig. 5. At 1σ, the NaIνE data imply $\sigma(0n) = (5.2^{+3.4}_{-3.1}) \times 10^{-40}$ cm^2 after profiling $\sigma(\geq 1n)$, consistent with Ref. [12] and MARLEY's prediction [18], though uncertainties are large due to the $\geq 1n$ events present in NaIνE. The determined 1σ range for $\sigma(\geq 1n)$ is $2.2^{+3.5}_{-2.2} \times 10^{-40}$ cm^2 is roughly $10\times$ lower than the MARLEY model, suggesting the suppression in the total rate relative to MARLEY is due to the modeling of the $\geq 1n$ channel. Profiles for the exclusive cross-section fits can be found in Supplemental Material [18], which includes Refs. [29–37].

Conclusion.—COHERENT has measured the inclusive ν_eCC-^{127}I cross section on ^{127}I between 10 and 55 MeV to be $(9.2^{+2.1}_{-1.8}) \times 10^{-40}$ cm^2. This measurement is roughly 41% of the nominal cross section from MARLEY and to date is the heaviest CC neutrino-nucleus cross section measured in this energy regime. One source of suppression could arise from a quenched value of g_A, and, while this value cannot be determined due to the lack of forbidden transitions in the MARLEY model, an upper limit of $g_{A,\text{eff}} \leq 0.97$ is set. COHERENT's $0n$ emission measurement is consistent with the exclusive channel reported by E-1213 and with that predicted by the MARLEY model. The fit to the $\geq 1n$ emission cross section is much smaller than predicted, similar to the suppression observed by COHERENT's previous measurement on lead. The

detector continues to collect data, and the future 3.5T NaIνETe detector will improve the current statistical limitations. There are additional efforts within the collaboration to utilize machine-learning approaches on NaIνE data to further improve signal to background. COHERENT's future inelastic detectors will study interactions on ^{2}H, ^{16}O, ^{40}Ar, and ^{232}Th, significantly increasing the number of neutrino-nucleus interactions studied at these energies.

---

[*] peibo.an@alumni.duke.edu

[†] hedges3@llnl.gov

[‡] Also at Lawrence Livermore National Laboratory, Livermore, California 94550, USA.

[§] Also at Lebedev Physical Institute of the Russian Academy of Sciences, Moscow, 119991, Russian Federation.

[‖] Also at University of Naples Federico II, Naples 80138, Italy.

[¶] Also at South Dakota School of Mines and Technology, Rapid City, South Dakota 57701, USA.

[**] Also at Fermi National Accelerator Laboratory, Batavia, Illinois 60510, USA.

[1] J. A. Formaggio and G. P. Zeller, Rev. Mod. Phys. **84**, 1307 (2012).

[2] R. Maschuw, B. Armbruster, G. Drexlin, V. Eberhard, K. Eitel, H. Gemmeke, T. Jannakos, M. Kleifges, J. Kleinfeller, C. Oehler *et al.*, Prog. Part. Nucl. Phys. **40**, 183 (1998).

[3] P. An, C. Awe, P. S. Barbeau, B. Becker, S. W. Belling, V. Belov, I. Bernardi, C. Bock, A. Bolozdynya, R. Bouabid *et al.*, Phys. Rev. D **108**, 072001 (2023).

[4] W. C. Haxton, Phys. Rev. Lett. **60**, 768 (1988).

[5] J. Engel, S. Pittel, and P. Vogel, Phys. Rev. C **50**, 1702 (1994).

[6] Y. S. Lutostansky, A. N. Fazliakhmetov, G. A. Koroteev, N. V. Klochkova, A. Y. Lutostansky, A. P. Osipenko, and V. N. Tikhonov, Phys. Lett. B **826**, 136905 (2022).

[7] T. S. Kosmas and E. Oset, Phys. Rev. C **53**, 1409 (1996).

[8] S. Mintz and M. Pourkaviani, Nucl. Phys. **A584**, 665 (1995).

[9] M. S. Athar, S. Ahmad, and S. Singh, Nucl. Phys. **A764**, 551 (2006).

[10] J. Engel and J. Menéndez, Rep. Prog. Phys. **80**, 046301 (2017).

[11] D. Akimov, J. B. Albert, P. An, C. Awe, P. S. Barbeau, B. Becker, V. Belov, A. Brown, A. Bolozdynya, B. Cabrera-Palmer *et al.*, Science **357**, 1123 (2017).

[12] J. R. Distel, B. T. Cleveland, K. Lande, C. K. Lee, P. S. Wildenhain, G. E. Allen, and R. L. Burman, Phys. Rev. C **68**, 054613 (2003).

[13] D. Akimov *et al.* (COHERENT Collaboration), Phys. Rev. D **106**, 032003 (2022).

[14] J. Amaré, S. Cebrián, I. Coarasa, C. Cuesta, E. García, M. Martínez, M. A. Oliván, Y. Ortigoza, A. O. de Solórzano, J. Puimedón *et al.*, Phys. Rev. Lett. **123**, 031301 (2019).

[15] H. Lee, B. J. Park, J. J. Choi, O. Gileva, C. Ha, A. Iltis, E. J. Jeon, D. Y. Kim, K. W. Kim, S. H. Kim *et al.*, Front. Phys. **11** (2023).

[16] D. W. Aitken, B. L. Beron, G. Yenicay, and H. R. Zulliger, IEEE Trans. Nucl. Sci. **14**, 468 (1967).

[17] R. P. Gardner and C. W. Mayo, Appl. Radiat. Isot. **51**, 189 (1999).

[18] See Supplemental Material at http://link.aps.org/supplemental/10.1103/PhysRevLett.131.221801 for a detailed explanation of calibrations and a differential cross section measurement.

[19] S. Gardiner, Comput. Phys. Commun. **269**, 108123 (2021).

[20] S. Gardiner, Phys. Rev. C **103**, 044604 (2021).

[21] M. Palarczyk, J. Rapaport, C. Hautala, D. L. Prout, C. D. Goodman, I. J. van Heerden, J. Sowinski, G. Savopulos, X. Yang, H. M. Sages *et al.*, Phys. Rev. C **59**, 500 (1999).

[22] N. Paar, T. Marketin, D. Vale, and D. Vretenar, Int. J. Mod. Phys. E **24**, 1541004 (2015).

[23] J. Rapaport, T. Taddeucci, T. Welch, C. Gaarde, J. Larsen, D. Horen, E. Sugarbaker, P. Koncz, C. Foster, C. Goodman *et al.*, Nucl. Phys. **A410**, 371 (1983).

[24] S. Agostinelli, J. Allison, K. Amako, J. Apostolakis, H. Araujo, P. Arce, M. Asai, D. Axen, S. Banerjee, G. Barrand *et al.*, Nucl. Instrum. Methods Phys. Res., Sect. A **506**, 250 (2003).

[25] V. Tretyak, Astropart. Phys. **33**, 40 (2010).

[26] R. L. Workman *et al.* (Particle Data Group), Prog. Theor. Exp. Phys. **2022**, 083C01 (2022).

[27] L. Schaller, J. Kern, and B. Michaud, Nucl. Phys. **A165**, 415 (1971).

[28] M. Islam, T. Kennett, and W. Prestwich, Z. Phys. A **335**, 173 (1990).

[29] T. Suzuki, D. F. Measday, and J. P. Roalsvig, Phys. Rev. C **35**, 2212 (1987).

[30] A. J. Koning, M. C. Duijvestijn, and S. Hilaire, *TALYS-10* (EDP Sciences, France, 2008), ISBN: 978-2-7598-0090-2,

nuclear physics and radiation physics, http://inis.iaea.org/search/search.aspx?orig_q=RN:41034220.

[31] T. Taddeucci, C. Goulding, T. Carey, R. Byrd, C. Goodman, C. Gaarde, J. Larsen, D. Horen, J. Rapaport, and E. Sugarbaker, Nucl. Phys. **A469**, 125 (1987).

[32] A. E. Champagne, R. T. Kouzes, A. B. McDonald, M. M. Lowry, D. R. Benton, K. P. Coulter, and Z. Q. Mao, Phys. Rev. C **39**, 248 (1989).

[33] J. Engel, S. Pittel, and P. Vogel, Phys. Rev. Lett. **67**, 426 (1991).

[34] P. Vogel, J. Engel, and S. Pittel, Nucl. Phys. **A577**, 425 (1994).

[35] J. N. Bahcall, E. Lisi, D. E. Alburger, L. De Braeckeleer, S. J. Freedman, and J. Napolitano, Phys. Rev. C **54**, 411 (1996).

[36] Y. Fujita, Y. Shimbara, I. Hamamoto, T. Adachi, G. P. A. Berg, H. Fujimura, H. Fujita, J. Görres, K. Hara, K. Hatanaka *et al.*, Phys. Rev. C **66**, 044313 (2002).

[37] H. Junde, H. Su, and Y. Dong, Nucl. Data Sheets **112**, 1513 (2011).

Correction: Uncertainties appearing in the last sentence of the abstract were incorrect and have been fixed.